Astron. Astrophys. 322, 266–279 (1997)

ASTRONOMY
AND
ASTROPHYSICS

The Na I $\lambda\lambda$5890,5896 resonance doublet as chromospheric diagnostics in M dwarfs

V. Andretta[1,2], **J.G. Doyle**[2], **and P.B. Byrne**[2]

[1] *Current Address:* NASA/GSFC, Laboratory for Astronomy and Solar Physics, Code 682, Greenbelt, MD 20771, USA
[2] Armagh Observatory, College Hill, Armagh BT61 9DG, Northern Ireland
(andretta@gsfc.nasa.gov, jgd@star.arm.ac.uk, pbb@star.arm.ac.uk)

Received 12 August 1996 / Accepted 22 November 1996

Abstract. The Na I D lines at 5890/5896 Å are very prominent features in the spectrum of late-type stars. Nevertheless, little attention has been devoted to the potential use of those lines as chromospheric diagnostics. As a case study, we explore the dependence on chromospheric activity of the D lines in a star with $T_{\rm eff}$ = 3700 K, $\log g$ = 4.7 and solar metallicity. The results are compared with the better studied hydrogen spectrum. We find that the D lines seem to be a promising diagnostic of the lower-middle chromosphere, that can complement the information given by lines like Hα. We also find that, for detailed quantitative studies, it is necessary to include a proper treatment of the background opacities. Less important, instead, is the need of careful treatment of transitions induced by collisions with hydrogen atoms. Finally, our calculations make it clear that, for the most active stars, the level of coronal emission should also be taken into account.

Key words: stars: late-type – stars: activity – stars: chromospheres – line: formation – radiative transfer

1. Introduction

The study by spectroscopic means of the chromospheres of late type stars relies heavily on strong lines of hydrogen or of abundant metals. The fact that chromospheres in solar-type stars consist of a rather tenuous plasma normally causes the source function of these lines to decouple from the local thermal pool in large parts of the line-forming regions. Hence significant departures from local thermodynamic equilibrium (LTE) affect the transfer of radiation in practically all chromospheric diagnostics.

From the classical theory of non-LTE transfer of line radiation, assuming the equality of the line absorption and emission profiles, the source function can be written (Thomas 1957, 1965) as

$$S = \frac{\bar{J} + \varepsilon B(T) + \eta B^*}{1 + \varepsilon + \eta}. \quad (1)$$

In this expression, the term $\bar{J}$, the specific intensity averaged over all directions and over the line profile, accounts for the non-coherent photon scattering, while the terms $\varepsilon B(T) + \eta B^*$ and $\varepsilon + \eta$ represent, respectively, the photon "source" and "sink" terms. In particular, the term $\varepsilon B(T)$ accounts for the creation of line photons by direct collisional excitation: it thus expresses the coupling of the source function with the local thermal pool ($B(T)$ is the Planck function relative to the local kinetic temperature T). Conversely, the term ε in the denominator of Eq. 1 is due to the destruction of photons by direct collisional deexcitation. The terms ηB^* and η include all other indirect processes. Usually, these latter terms are dominated by bound-free processes, and B^* can be expressed as the Planck function at the radiation temperature of the relevant continuum. Thus, if $\eta B^* > \varepsilon B(T)$ and $\eta > \varepsilon$ the line is said to be "photoionisation dominated"; vice versa, when the opposite inequalities hold, the line is "collision dominated". All other cases lead to "mixed domination".

It is clear from Eq. 1 that whenever direct collisional processes dominate over scattering and indirect excitation/deexcitation processes, the line source function approaches LTE. On the other hand, the decoupling from the chromospheric thermal pool, i.e. the departure of the line source function from $B(T)$, can be rather extreme. For example, the strong resonance lines classified as photoionisation dominated are rather insensitive to the chromospheric temperature rise, even if their cores are formed in the chromosphere: on the contrary, they are controlled by a photoionising radiation field that forms in other atmospheric layers, normally the photosphere. In the solar atmosphere, the Na I D resonance doublet at 5890/5896 Å is usually regarded as an example of such a "bad" chromospheric diagnostic, as opposed, for instance, to the collision dominated resonance lines of Ca^+ or Mg^+. In this case, the radiation field

Send offprint requests to: V. Andretta

that dominates the formation of the line is the photospheric ultraviolet radiation shortward 2413 Å, the photoionisation threshold of Na^0. This is because the main source term in Eq. 1, ηB^*, is due to the feeding of level $3p$ (the upper level of the D doublet) through the path $Na^0\ 3s \rightarrow Na^+ \rightarrow Na^0\ 3p$. It is perhaps this kind of consideration that justifies the relative paucity of work done on the Na I D lines in the study of the chromospheres in late type stars (notable exceptions are Sakhibullin 1987 and Thatcher 1994).

Nevertheless, it should be noted that, as the physical properties of the stellar atmosphere change, a line can switch category with respect to its solar classification. In particular, the UV radiation field in very cool stars is much less intense than in the Sun, and that may make possible a collisional control of the D lines. Moreover, the relatively high density of the chromosphere of cool dwarfs may tend to enhance this effect. It is true that, even in some M stars, low resolution spectra of the D lines do not show core emission (Pettersen & Hawley 1989), the signature of the chromospheric temperature rise in collisionally controlled lines. But high spectral resolution observations of active M dwarfs do in fact reveal the presence of an emission in the core of the Na I doublet (see e.g. Pettersen 1989, or Panagi et al. 1991). This chromospheric feature is not as spectacular as the emission of, say, Hα or Ca II H & K; on the other hand, the Na I D doublet presents some distinct advantages as a diagnostic that we will investigate in this paper (see also last paragraph of Sect 2.1).

While a more detailed comparison with chromospheric diagnostics other than hydrogen lines is outside the scope of this study, from an observational standpoint an obvious advantage of the Na I doublet is that it lies in a region where M dwarfs are considerably brighter (even an order of magnitude or more) than at the wavelengths of the Ca II and Mg II resonance lines. Also, most current ground-based instrumentation is more sensitive in the V band. Finally, it is worth mentioning that the interesting chromospheric/transition region He I λ5876 line (D_3) happens to be very close in wavelength to the Na I doublet. Indeed, we feel that observations of the D lines together (Na I $D_1 + D_2$ and He I D_3) provide a relatively easy-to-get and potentially very useful data-set.

We will, however, compare more in detail the formation of the Na I D doublet with the hydrogen line spectrum. As an introductory remark, here it is opportune to note only that there is a consensus on the fact that Hα in cool dwarfs is completely uncoupled from the thermal structure of the region at the temperature minimum (Cram & Mullan 1979, henceforth: CM). In fact, in M dwarfs that line is a good diagnostic of the upper chromosphere (Houdebine & Doyle 1994). The Na I D doublet in M dwarfs on the other hand displays well developed photospheric wings. It is therefore reasonable to expect that its profile can map the entire atmosphere from the photosphere up to the chromosphere, including the region of temperature minimum not covered by Hα. It has in fact been shown (Caccin et al. 1993, henceforth: CGS) that in sunspot umbrae (i.e. in conditions that approach those of late-type stars), the Na I D doublet is a good diagnostic of the thermal structure close to the temperature minimum.

2. Method

In order to examine in detail the formation of the Na I D doublet in cool dwarfs, rather than making an extended study across the HR diagram, we focussed our attention on a specific case. Starting from a photosphere representative of an early M dwarf, we then added a grid of model chromospheres (Sect. 2.2). For each model atmosphere we computed the emerging Na I spectrum using a non-LTE radiative transfer code, MULTI (Carlsson 1986), version 2.0. The code has been modified in several respects, mostly to deal with the overlapping (severe in late-type stars) of the fine structure components in most of the Na I lines, including the resonance doublet at 5890/5896 Å. The treatment of the boundary conditions (Sect. 2.3) and of the background atmospheric opacity (Sect. 2.4) has also been improved. For the line scattering process, the code employs the approximation of complete frequency redistribution of photons within the line profile (CRD).

For each model chromosphere, i.e. for each temperature structure, the electron density, proton density etc., were set to a first guess. A self-consistent solution was then found by solving the non-LTE problem for hydrogen and iterating to include the equation of hydrostatic equilibrium, taking into account the departures from LTE of sodium. As a by-product of this procedure, along with the sodium lines, we simultaneously obtain the hydrogen spectrum. This provides the opportunity to compare the Na I lines with other chromospheric diagnostics, such as Hα. The results are discussed in Sect. 3; in the following sections we will describe the procedures employed in the calculations.

2.1. Model atoms

The H model atom comprises 9 levels plus continuum. The transfer of radiation in all the radiative transitions (36 lines and 9 continua) was explicitly computed in non-LTE. The collisional bound-bound and bound-free cross-sections used in the rate equations are from Johnson (1972).

The Na model atom used in our calculations has been derived essentially from CGS and Bruls et al. (1992); its term structure includes 10 bound levels (up to n=7; some of the highest lying terms were grouped together), plus the ground states of Na^+ and Na^{++}.

It is usually assumed that electrons give the main contribution to collisional transition rates in stellar atmospheres. However, in cool atmospheres the electron density can be so low that other perturbers may become important, hydrogen in particular. We have followed CGS in their adaptation of the cross sections of Kaulakys (1985, 1986) for the excitation of the first 6 levels of Na by collisions with hydrogen atoms. The Kaulakys formula, valid for Rydberg atoms, is expected to give fair estimates for alkali atoms. An alternative approach following Drawin (1968, 1969), generalised by Steenbock & Holweger (1984) and, for forbidden transitions, by CGS, leads to cross

sections that are usually much larger, even by a factor 10^3. However, there are indications that the latter cross-sections may be strongly overestimated (CGS, Pavlenko & Magazzù 1996, and references therein). We therefore adopt the cross-sections from the Kaulakys approach, but in Sect. 3.3 we will also compare the results obtained with the Drawin formulae for a sample model. For a more detailed discussion on the Kaulakys and Drawin rates we refer to CGS. We feel we should only mention here that their Eq. 1 presents several typographical errors, that however do not reflect errors in their actual calculations.

One of the main differences with the previous Na model atoms, is the fact that we accounted for the fine structure of almost all the transitions in the model atom. The oscillator strengths for the fine structure components in the line have been computed from the total oscillator strength of the transition assuming LS coupling. Moreover, in the calculation of the line profiles we assumed that the relative populations of the sublevels are proportional to their degeneracies. This approximation also considerably simplifies the rate equations.

Another difference is the inclusion of a further stage of ionisation (Na^{++}). Given the combined effect of the low ionisation potential of Na^0 (5.139 eV) and of the high ionisation potential of Na^+ (47.286 eV), sodium is mostly in the form of Na^+ in the photosphere and chromosphere of solar-type stars. However, in active stars, the wavelength range below the photoionisation threshold for Na^+ (262 Å) is rich with coronal emission lines. Since it is not evident a priori that such a coronal illumination has no influence on the ionisation balance of sodium in the chromosphere, we have studied this effect in some of the models. Hence the necessity of including at least the ground state of Na^{++} in the model atom. For the ground state of Na^+ the photoionisation cross-section was obtained from the Opacity Project database (e.g. Seaton 1987; calculations by Scott 1996), while the collisional ionisation rate is from Landini & Monsignori Fossi (1990);

As for the treatment of the transfer of line radiation in the Na I D lines, the approximation of CRD is adequate, at least in main-sequence stars (Kelch & Milkey 1976). From a computational point of view, this is a considerable simplification with respect to the more general case of partial redistribution (PRD). This fact may be regarded as an advantage for the D lines over other more widely used chromospheric diagnostics (e.g Ca II or Mg II resonance lines), for which CRD is not as good an approximation.

2.2. Model atmospheres

The model photosphere, from Allard & Hauschildt (1995b), corresponds to a star with effective temperature $T_{\rm eff}$ = 3700 K, $\log g$ = 4.7 (g, gravity acceleration, in cm s^{-2}) and solar metallic abundances. The model belongs to version 5 (in preparation) of the grid obtained with Allard & Hauschildt's code PHOENIX. Such a grid of models differs from the previous one (Allard & Hauschildt 1995a) in several aspects, notably in improved molecular opacities.

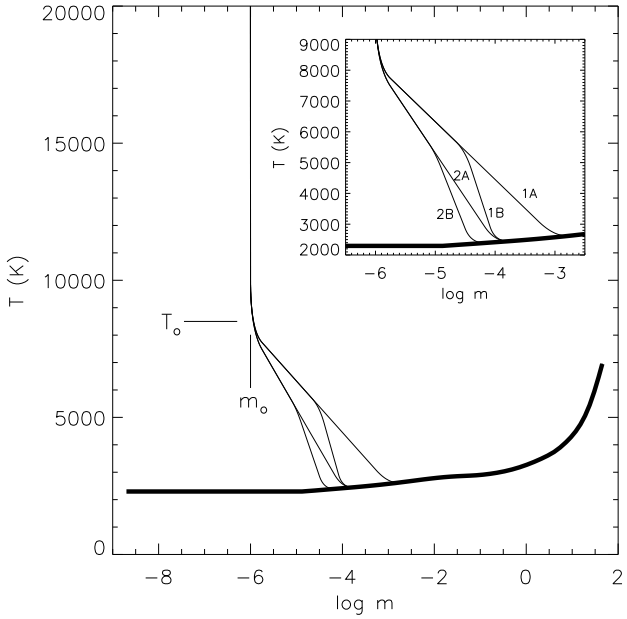

Fig. 1. Four chromospheric structures we have grafted to the photospheric structure of Allard & Hauschildt (1995b). For these models, the transition region starts at $\log m_\circ = -6$. Each chromospheric structure is labeled in the close-up plot; see text for an explanation of labeling. The base model photosphere is designated by a thick solid line.

We have superimposed to that base photosphere a grid of model chromospheres, each one described by an ad hoc thermal structure $T(\log m)$ (m is the column mass, in g cm^{-2}). At a given position of the onset of the transition region, specified by the pair $(T_\circ, m_\circ)$, we have considered four types of chromospheric thermal stratification, as in Fig. 1. Models $1A$ and $2A$ are constructed using segments where the temperature varies linearly with $\log m$. Models B ($1B$ and $2B$) are identical to the corresponding A models in the upper chromosphere, while the temperature gradient in the lower chromosphere has been steepened, causing the temperature minimum to be pushed further out. The main reason for this choice of models is that we want to probe the sensitivity of Na I lines to the structure of the lower chromosphere.

In the construction of the models, another relevant parameter is the temperature gradient in the transition region. Again, we have chosen to assume a linear dependence of T with $\log m$, or a constant gradient $\nabla_{\rm TR}\, T \equiv |{\rm d}T/{\rm d}\log m|$. For a given chromospheric structure, we have considered the values $\log \nabla_{\rm TR}\, T$ = 6.5 and 7, thus bringing to eight the number of model atmospheres at a given position of the onset of the transition region.

As for $T_\circ$, we fixed its value to 8500 K, following Houdebine & Doyle (1994). More important in determining the "activity" of a model chromosphere is its pressure. Following the procedure outlined by Andretta & Giampapa (1995), we generate more "active" states from a given "quiet" chromosphere by translating the temperature structure toward higher mass columns. Thus, the variation of the pressure in the chromosphere and

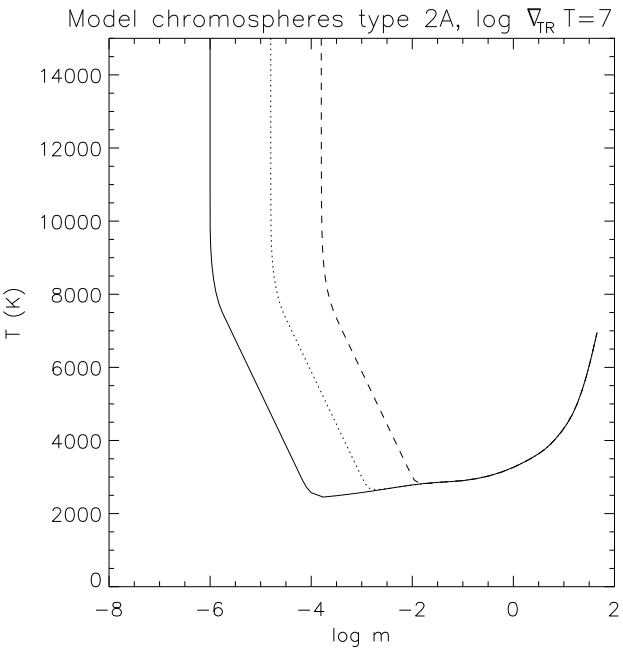

Fig. 2. Run of temperature for three models belonging to the series of model chromospheres generated (see text) from a chromosphere structure of type $2A$ (see Fig. 1) and $\log \nabla_{\rm TR}\, T = 7$. The three models shown here correspond to $\log m_\circ = -6.0$ (solid line), -4.8 (dotted line) and -3.8 (dashed line).

transition region can be conveniently parametrised by the mass loading at the top of the chromosphere, $m_\circ$. More specifically, we considered the models with $\log m_\circ = -6$ as being representative of a quiet chromosphere. We then generated a series of more active models by increasing the mass loading up to $\log m_\circ = -3.8$. In particular, nine values of $\log m_\circ$ spanning this interval were considered. This procedure has been followed for each one of the eight "basic" models we have already described, thus obtaining eight series of model atmospheres, for a total of 72 chromospheric structures. As an example, Fig. 2 shows three sample models belonging to the series with chromosphere structure of type $2A$ and $\log \nabla_{\rm TR}\, T = 7$.

Note that, in hydrostatic equilibrium, the gradient $\nabla_{\rm TR}\, T$ is related to the gradient $\mathrm{d}T/\mathrm{d}h$ (h is the height above the photosphere) via the equation: $\nabla_{\rm TR}\, T = H\, \mathrm{d}T/\mathrm{d}h\, \ln 10$, where H is the pressure scale height, which depends only on temperature and on the molecular mean weight. Therefore, the adopted scaling with $m_\circ$ preserves $\mathrm{d}T/\mathrm{d}h$ in the transition region and, less accurately, in the chromosphere (the mean molecular weight in the transition region is practically constant, whereas in the upper chromosphere it depends, among the other things, on the non-LTE ionisation equilibrium of hydrogen).

Microturbolence, ξ, is another ingredient in the construction of the model atmospheres, if less important than the temperature structure. In the photosphere we adopted a constant value $\xi_{\rm ph} = 1$ km/s. In the chromosphere we gradually increased the magnitude of the microturbolence field as $[\xi_{\rm ph} + (m_{\rm min}/m)^{1/5} - 1](T/T_{\rm min})^{1/2}$, where $m_{\rm min}$ is the location of the temperature minimum, and $T_{\rm min}$ is the corresponding value of temperature. This function roughly matches the distribution in the standard solar model chromosphere from Vernazza et al. 1981, but it is otherwise arbitrary. For most part of the model chromospheres, the resulting microturbolence does not exceed a few kilometers per second, up to about 5 km/s at $T_\circ$ in models 1B, 2A and 2B. For the non-quiescent models the same scaling with $m_\circ$ as for the temperature distribution has been adopted.

2.3. Coronal back-radiation

As anticipated in Sect. 2.1, the presence of often vigorously active coronae in chromospherically active stars can potentially affect the ionisation equilibrium of sodium. In fact, the structure of the transition region and upper chromosphere in M dwarfs can be altered by coronal back-radiation (Cram 1982). However, we will not deal explicitly with the problem of determining the structure of an X-ray illuminated atmosphere. Rather, we will limit ourselves to the simpler problem of determining the ionisation equilibrium of sodium in the presence of an XUV flux capable of ionising Na^+.

In order to study this problem, parallel to the model calculations with the temperature structures determined as described in the previous section with no coronal illumination, we have also considered the case of a non-zero coronal flux as a boundary condition atop the model atmosphere.

The spectrum of the coronal flux in the XUV below 262 Å, the photoionisation threshold for Na^+, has been obtained from the observed solar irradiance at activity minimum, as modelled by Tobiska (1991). These intensities, representative of an "average" solar quiet corona, have been multiplied by a factor 10^4; the result is shown in Fig. 3. The corresponding surface total flux in the soft X-band 0.15–4.0 keV is $\log F_{\rm X} = 7.35$ ($F_{\rm X}$ in ergs cm^{-2} s^{-1}); assuming a radius $R = 0.7\, R_\odot$, and a corona homogeneously distributed over the stellar surface, the resulting total luminosity in the same band is $\log L_{\rm X} = 29.8$, while its ratio to the bolometric luminosity (for $T_{\rm eff} = 3700$ K) is $\log L_{\rm X}/L_{\rm bol} = -2.68$. These values correspond to a corona of a considerably active M star (Doyle & Butler 1985). Therefore they are intended to be used for upper-limit estimates of the effect of coronal radiation on the sodium spectrum.

2.4. Background opacity

We have already emphasised that the photospheric radiation field in the ultraviolet can be crucial in determining the formation of the Na I D line cores and, more generally, of the Na I spectrum in the presence of a chromosphere. Moreover, the resonance doublet exhibits remarkably broad wings in M dwarfs, that can span tens of Ångströms, an interval over which noticeable changes in the photospheric emission can occur. It is thus important to correctly evaluate the background photospheric emission.

The non-LTE code used here, MULTI, evaluates the photospheric radiation field from a given model atmosphere using

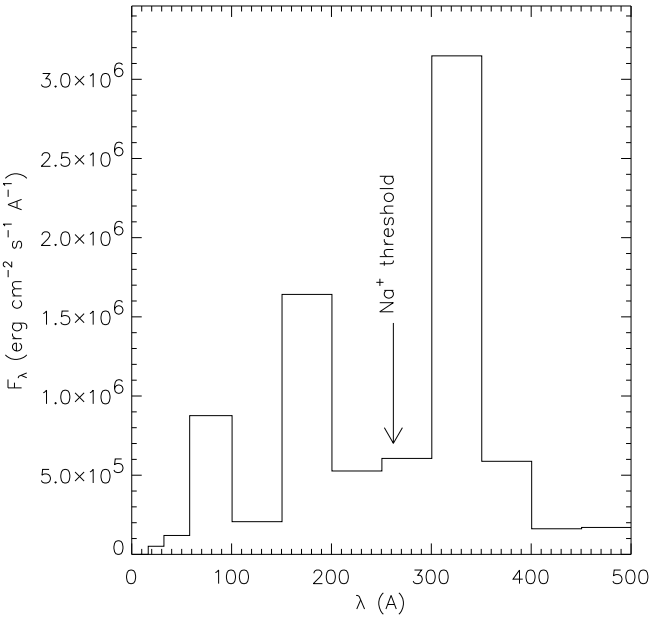

Fig. 3. Adopted coronal XUV distribution; the photoionisation threshold for Na^+ is also marked.

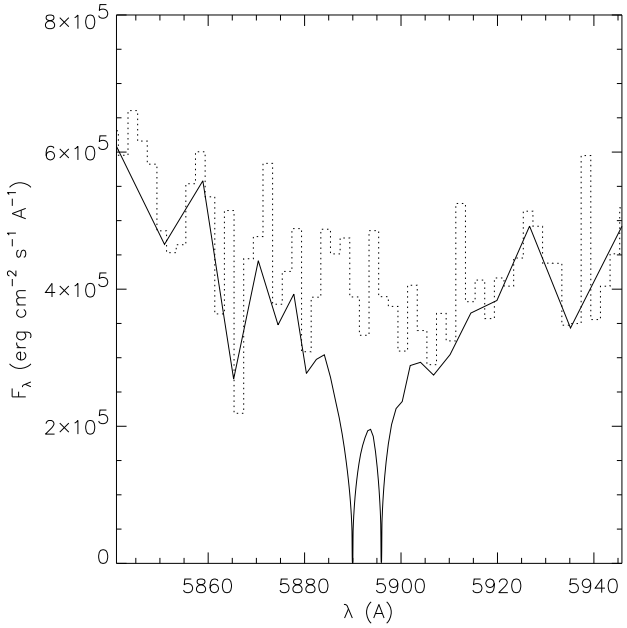

Fig. 4. The D lines computed from the model photosphere of Allard & Hauschildt (1995b). The dotted histogram represent the "background" photospheric flux (see text).

a variety of continuum opacity sources. In M dwarfs, however, a very large number of atomic and molecular lines gives an important, even dominant contribution, to the plasma opacity. Therefore, we have added to the "standard" MULTI calculations, opacities from atomic and molecular lines in the form of an opacity table, provided again by Allard & Hauschildt (1995b) along with their atmospheric model (see Sect. 2.2).

In the table, the opacity dependence upon wavelength is given at each depth point of the model atmosphere with a step of 2 Å. Such a wavelength sampling is adequate for the calculations of photoionisation and photoexcitation rates, and for a comparison of the resulting synthetic spectra with low resolution observations.

One difficulty is that the opacity data used here are model-specific. However, in the model atmospheres constructed as described in Sect. 2.2, the photosphere is left unaltered. Therefore, in that region it is still correct to use the tabulated additional opacities. For the higher chromospheric temperatures, the standard MULTI background opacities were used. Thus, in our calculations we have included the additional background opacities only in the photosphere, that is, in the region below the temperature minimum. Above that region, the additional opacities have been ignored, except for a smooth "transition" region, spanning a decade in column mass. Such a smooth zeroing of the additional line opacities has been introduced in order to mimic the dissociation of molecular species in the chromosphere (for this specific model, molecules are the main contributor to the total opacity in the temperature minimum region and for most parts of the photospheric spectrum).

Another problem that requires a proper treatment of plasma opacity, is the transfer in the chromosphere of XUV photons below the Na^+ photoionisation threshold. In addition to the H and He opacities already included in the code, we have taken into account inner-shell photoionisation by the most abundant metals, following Avrett & Loeser (1988).

3. Results and discussion

In the following discussion about the effect of a chromosphere on the D lines, we will often use the line profile produced by the photosphere alone as a reference. Fig. 4 shows such an emerging profile as computed with the adopted model photosphere. For the sake of consistency, the electron density has been recomputed following the same procedure, outlined in Sect. 2, as used for the model chromospheres. The resulting electron densities differ from the tabulated values by at most a few percent. The Na I and H I line profiles calculated from that purely photospheric model, will hereafter be referred to as the "photospheric" profiles.

The same figure also shows the "background" photospheric spectrum, at the resolution dictated by the input opacity tables (2 Å). Such a background spectrum represents the emerging spectrum obtained ignoring line absorption by sodium atoms; the variations in the background opacity affecting the wings of the D lines are readily apparent. Note also the severe blending between D_1 and D_2, which justifies our treatment of line overlapping (Sect. 2.1).

3.1. Dependence on atmospheric density and structure

We now proceed by first examining the effect of the structure of the chromosphere on the H I and Na I line spectrum. In the

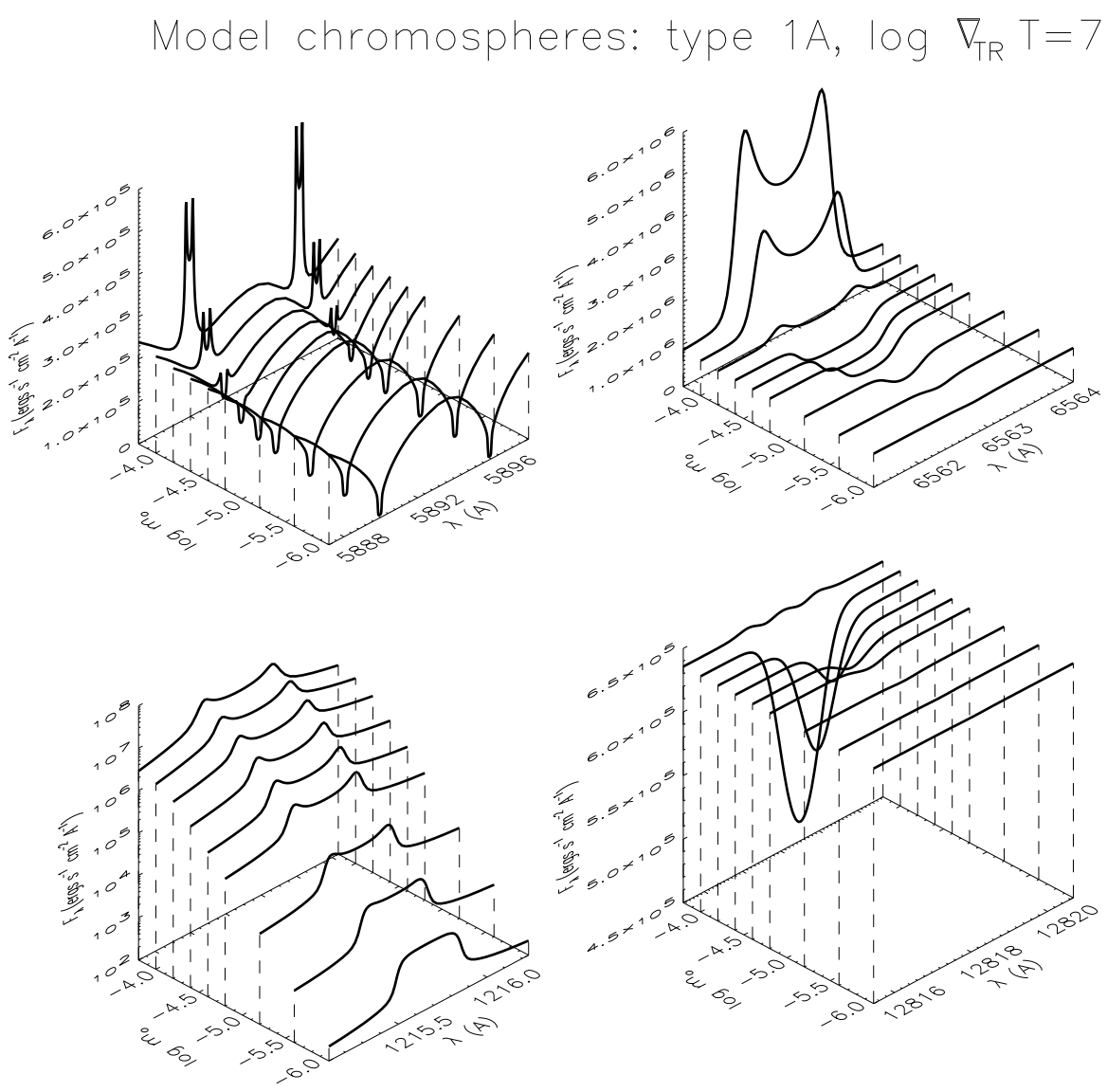

Fig. 5. Dependence upon the parameter $m_\circ$ of some features of the Na I and H I spectra: the core of Na I D_2 and D_1 (upper-left panel), Hα (upper-right panel), Lyα (lower-left panel), Paβ (lower-right panel). The line profiles correspond to model chromospheres type 1A (see Fig. 1). Note the logarithmic scale for the Lyα flux. For each profile, a dashed line indicates the corresponding value on the $\log m_\circ$ axis.

following sections we will deal with the other aspects we anticipated in Sect. 2 to be relevant for our discussion, namely the presence of an active corona (Sect. 3.2) and the importance of a correct treatment of collisions with hydrogen (Sect. 3.3) and of background opacities (Sect. 3.4).

3.1.1. Dependence on atmospheric density

As discussed in Sect. 2.2, one of the main parameters characterising our model chromospheres is the pressure atop the chromosphere or, equivalently, the column mass at the onset of the transition region, $m_\circ$. Fig. 5 shows the dependence of Na I D lines and of some H I spectral features (Lyα, Hα, Paβ) upon this parameter, for a particular series of models (see figure caption). Along with Hα, we have chosen Paβ as a representative subordinate H I line instead of Paα because, due to strong telluric absorption, the latter is practically unobservable from Earth.

The approximation of CRD, used in our calculations, is poor in the wings of Lyα. Therefore, the Lyα profiles shown here are purely indicative. However, the total flux in the line, dominated by the line core, can be regarded as more reliable. As is clear from Fig. 5, the latter quantity increases monotonically with $m_\circ$: in fact, it increases approximately as its square. This scaling law can be understood considering that Lyα forms mainly in the transition region within a limited temperature range whose lower and upper boundaries are defined, respectively, by the rapid decrease of the collisional excitation rate of level $n = 2$ and by the complete ionisation of hydrogen. Moreover, in all but the most active models the Lyα line is effectively optically thin: in other words, practically all the photons created in the line

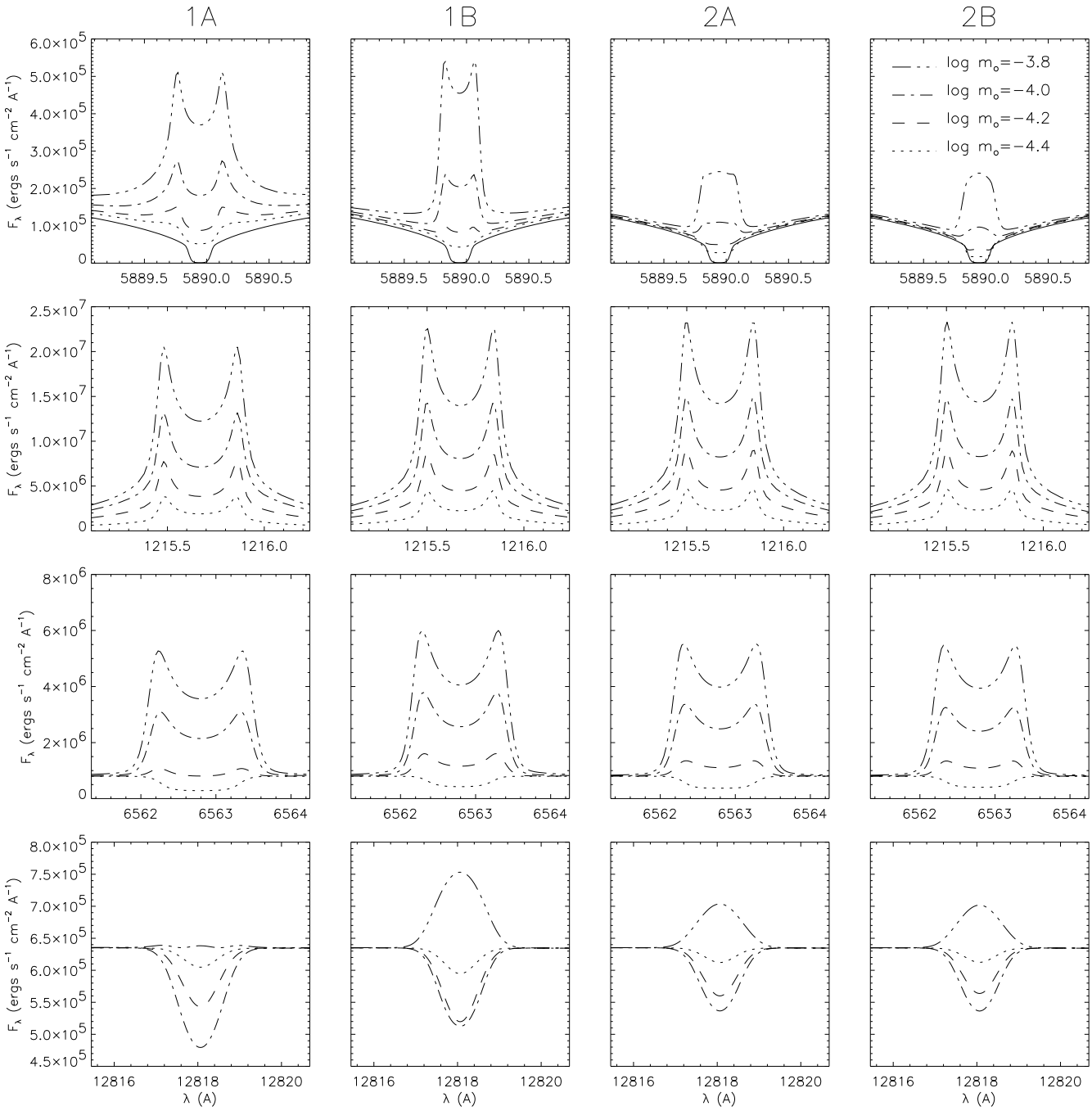

Fig. 6. Line profiles for the most active models of the four series of models with $\log \nabla_{\rm TR}\, T = 7$. From top to bottom: Na I D_2, Lyα, Hα, Paβ. For the Na I D_2 line the purely photospheric profile is also shown (solid line).

will eventually escape, possibly after multiple scatterings. The peak value of the source function (and of the emerging intensity, from the Eddington-Barbier relation) of a Doppler broadened line forming in an effectively thin, isothermal slab scales as $\varepsilon\tau_\circ$ (Athay 1972, p. 64), where ε is the collisional coupling parameter (see Eq. 1) and $\tau_\circ$ is the slab total optical thickness at the line center. Both ε and $\tau_\circ$ depend linearly on density: hence the quadratic dependence on $m_\circ$. The optical depth $\tau_\circ$ depends also on the gradient of the transition region, but we recall that within each series the models are scaled so that $\mathrm{d}T/\mathrm{d}h$ in the transition region is kept constant (see Sect. 2.2).

Similarly, starting from an almost zero core flux in the photospheric profile, the core of the D lines shows a monotonic increase with chromospheric pressure, with self-reversed emission in the most active models. By contrast, both Hα and Paβ, practically absent from the photospheric spectrum, show at first a deeper absorption against the photospheric background, and are eventually quickly driven into emission, at $\log m_\circ \approx -4$.

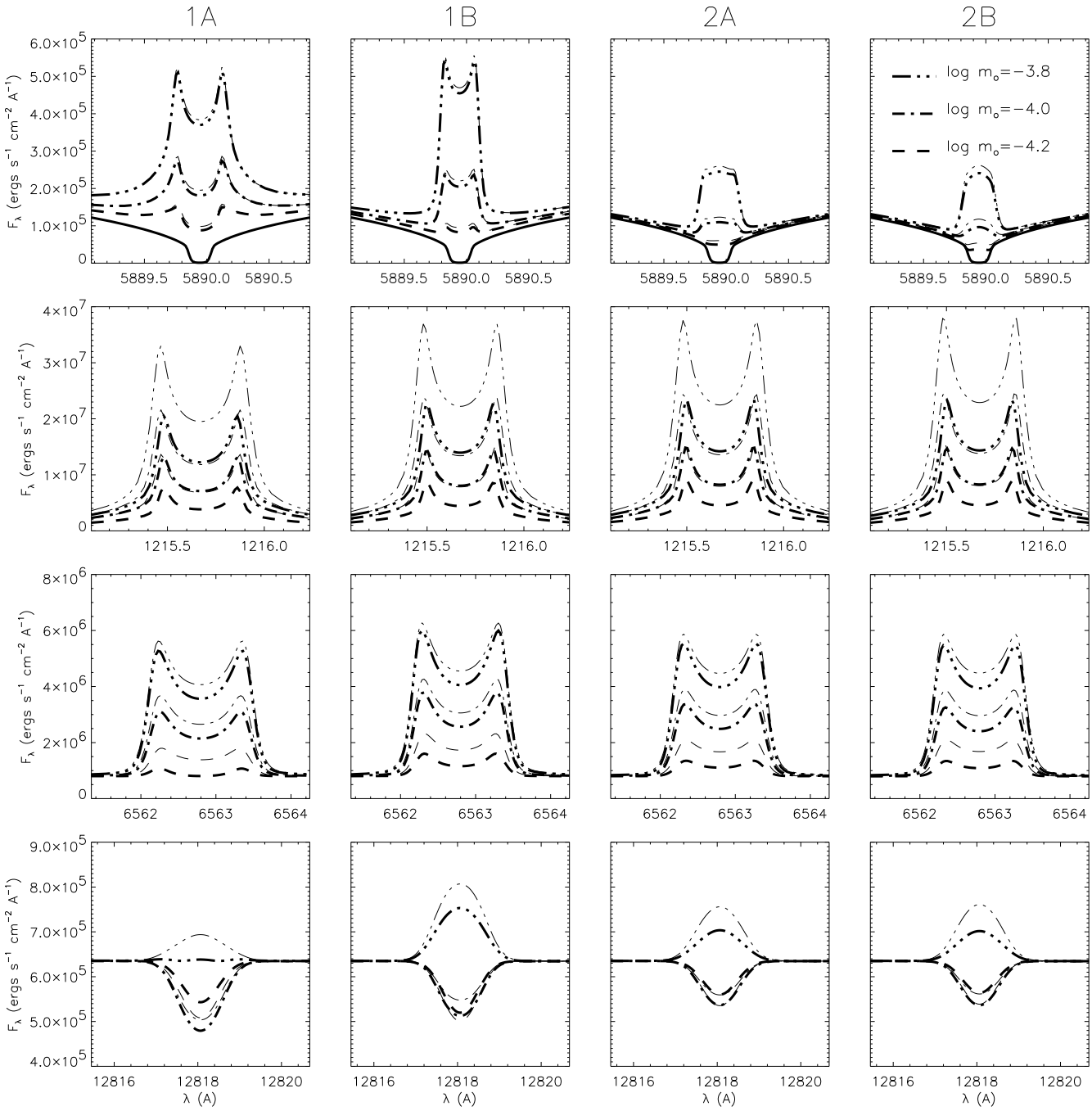

Fig. 7. Dependence on the gradient of the transition region. The thicker lines correspond, as in Fig. 6, to $\log \nabla_{\rm TR}\, T = 7$; the thinner lines to $\log \nabla_{\rm TR}\, T = 6.5$. Only the last three models in each series are shown in this figure.

The precise value of this "critical" pressure depends somewhat on the particular series of models and on the line: in our series of models, Hα tends to be driven into emission at $\log m_\circ$ between -4.4 and -4.2, while Paβ is driven into emission at $\log m_\circ \approx -3.9$. Such a "non-LTE curve of growth" has been noticed by CM for Hα, but is common to other H I subordinate lines.

3.1.2. Dependence on temperature structure

Fig. 5, while informative about the general trends as chromospheric activity increases, refers only to a specific temperature stratification in the chromosphere. Fig. 6 shows instead the consequences of differences in temperature structure on the same Na I and H I lines as the previous figure. For clarity, only the results for the last four models of each series are shown. As for the two D lines, only the core of D_2 is displayed in Fig. 6; the

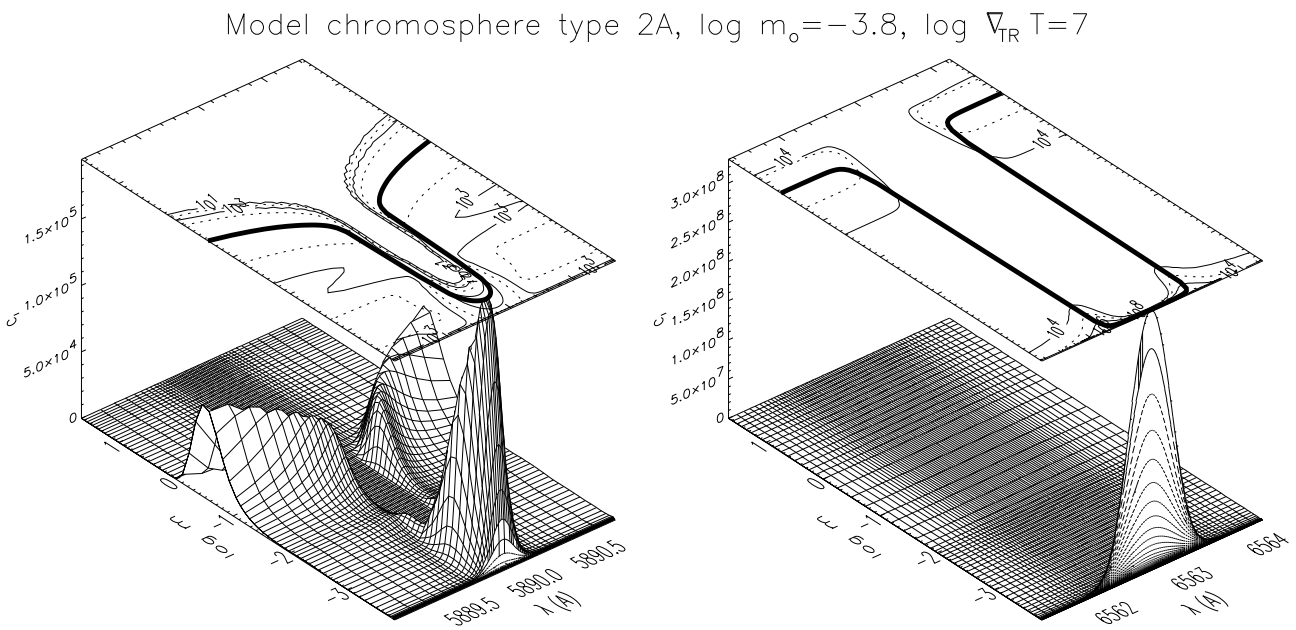

Fig. 8. Contribution functions, C_I, for intensity emerging at $\mu = 1$, as functions of wavelength and depth, for the core of D_2 (left) and Hα (right), in the model atmosphere with chromosphere type 2A, $\log m_\circ = -3.8$ and $\log \nabla_{\rm TR}\, T = 7$. In each panel, the contribution function is also shown with a contour plot; on the same graph the locus $\tau_\lambda = 1$ is drawn with a solid, thick line.

behaviour of D_1 is similar. Moreover, the photospheric profile is also plotted for comparison.

The Lyα line seems insensitive to the chromospheric structure, a fact consistent with the picture of a collisionally dominated line forming in the transition region. To a large extent the same can be said of the subordinate H I lines when in emission. In this case, density (or pressure, parametrised, as usual, by $m_\circ$) seems to be the most important parameter (CM, Cram & Mullan 1985, have investigated such a dependence for Hα).

Far more pronounced is the effect of the chromospheric structure on the D_2 line. In particular, it is interesting how the position of temperature minimum leaves its signature on the profile, mainly on the dip between the emission core and the photospheric wings (compare, for example, the profiles of models $1A$ with those of models $1B$). This is reminiscent of the effect on the Ca II H & K lines. From a computational point of view, however, the D doublet has the advantage over the Ca II lines that its profile is not affected by PRD problems (a fact already mentioned in Sect. 2.1).

For the most active models, at a given value of $m_\circ$ the extension of the chromosphere seems to be the dominant effect on the profile of the emission cores, as hinted by the systematic changes in the inner-core profiles from models $1B$ (the thinnest chromospheres) to models $1A$ (the thickest chromospheres). In fact, it is easy to see the progression from the round-top, gaussian-like profiles of models $2B$, through the flat-top profiles of models $2A$, to the self reversed profiles of models $1B$ and $1A$.

3.1.3. Dependence on the gradient of the lower transition region

To complete our investigation on the effect of the temperature structure, it remains to be examined how the lines we have considered respond to changes in the gradient (i.e. thickness) of the transition region. For this purpose, Fig. 7 displays the line profiles for the most active models (the last three models of each series, in this case), both for $\log \nabla_{\rm TR}\, T = 7$, as in Fig. 6, and for $\log \nabla_{\rm TR}\, T = 6.5$.

In the case of Lyα, it is interesting to note how a temperature gradient change in the transition region appears to be equivalent to a pressure change. For example, the profiles with $\log \nabla_{\rm TR}\, T = 6.5$ and $\log m_\circ = -4.0$ nearly overlap with the profiles with $\log \nabla_{\rm TR}\, T = 7$ and $\log m_\circ = -3.8$. This fact fits in the picture sketched above of a collisionally controlled Lyα whose main dependence is upon the temperature gradient (through the total optical depth of the emitting slab, $\tau_\circ$), as well as on the square of pressure. Thus, increasing the pressure in the transition region by 0.2 dex (the step between the models shown here) produces an increase of 0.4 dex in Lyα emission, almost equivalent to the change produced by the increase of the temperature gradient (0.5 dex).

The subordinate H I lines are less sensitive to changes in the transition region. This is consistent with the findings of Houdebine & Doyle (1994), but the effect of the gradient in the transition region cannot be neglected. In contrast, the D_2 line (and D_1, as well) is almost insensitive to the structure of the transition region. This implies that the core of the Na I lines forms at lower heights than the H I spectrum.

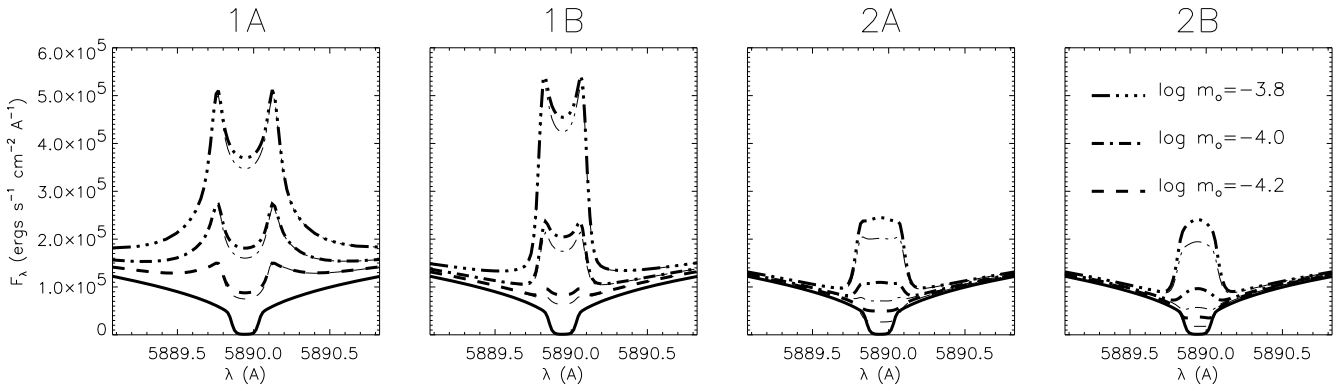

Fig. 9. D_2 core profiles for $\log \nabla_{\rm TR}\, T = 7$ (thick lines) compared with the results obtained with the coronal illumination of Fig. 3 (thin lines). As in preceding figures, the photospheric line profile is drawn with a solid line.

3.1.4. The region of formation of the D lines

The statement made at the end of the previous section, can be expressed in pictorial terms by the use of contribution functions. One possible definition of contribution function can be derived from the formal solution of the transfer equation for intensity in plane parallel, semi-infinite atmospheres. In this case, the contribution function, C_I, at each wavelength, λ, and cosine of the angle with the normal to the surface, μ, is defined so that:

$$I(\lambda, \mu) = \int C_I(\lambda, \mu, x)\, \mathrm{d}x,$$

where x is a depth coordinate. With the choice $x = \log m$, the contribution function becomes:

$$C_I = \frac{m}{\rho}\, \eta\, \mathrm{e}^{-\tau}\, \ln 10, \qquad (2)$$

where ρ is the density, η is the emissivity and τ is the optical distance to the surface. While alternative, more sophisticate definitions can be adopted (e.g. Magain 1986), Eq. 2 is sufficient for our purposes.

With the definition of contribution function given by Eq. 2, Fig. 8 summarises the main differences between the D lines and Hα and, by extension, all H I subordinate lines. As an example, we consider an active model ($\log m = -3.8$) with a chromosphere type 2A and $\log \nabla_{\rm TR}\, T = 7$. In this case the contrast between Hα and D_2 is immediately apparent. The former is exclusively formed in the upper chromosphere, while the core of the latter forms throughout almost the entire chromosphere. Only a small contribution to the D_2 emission, even for this very active model, comes from the lower transition region.

It should be remarked, however, that Eq. 2, as all the contribution functions proposed so far, is based on the *formal* solution of the transfer equation, which means that the source function and optical depth are considered as given quantities. It thus ignores the non-linear, non-local nature of radiative transfer in these strong lines, as well as the inter-dependence between different transitions. Therefore, while contribution functions can serve to illustrate some specific points, they cannot be a substitute of a more physically sound approach. Such an approach requires the study of the *response* of the emerging profile to variations of physical properties of the atmosphere, as we have done earlier in this section, and as we intend to do in the following discussion.

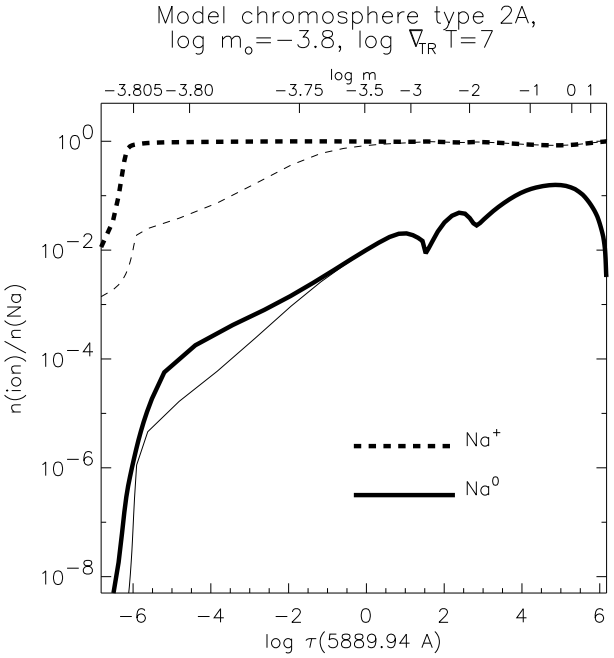

Fig. 10. Fractional abundances of Na^0 (solid lines) and Na^+(dashed lines), in the case of a model chromosphere type 2A, $\log m_\circ = -3.8$ and $\log \nabla_{\rm TR}\, T = 7$. Thicker lines refer to a null coronal illumination, while thinner lines represent abundances calculated with the XUV flux of Fig. 3. All quantities are plotted versus the optical depth at the central wavelength of the D_2 line.

3.2. Dependence on coronal illumination

The response of the D lines to coronal illumination is one possible non-local effect that is of interest. Fig. 9 compares some "standard" results presented so far with results obtained consid-

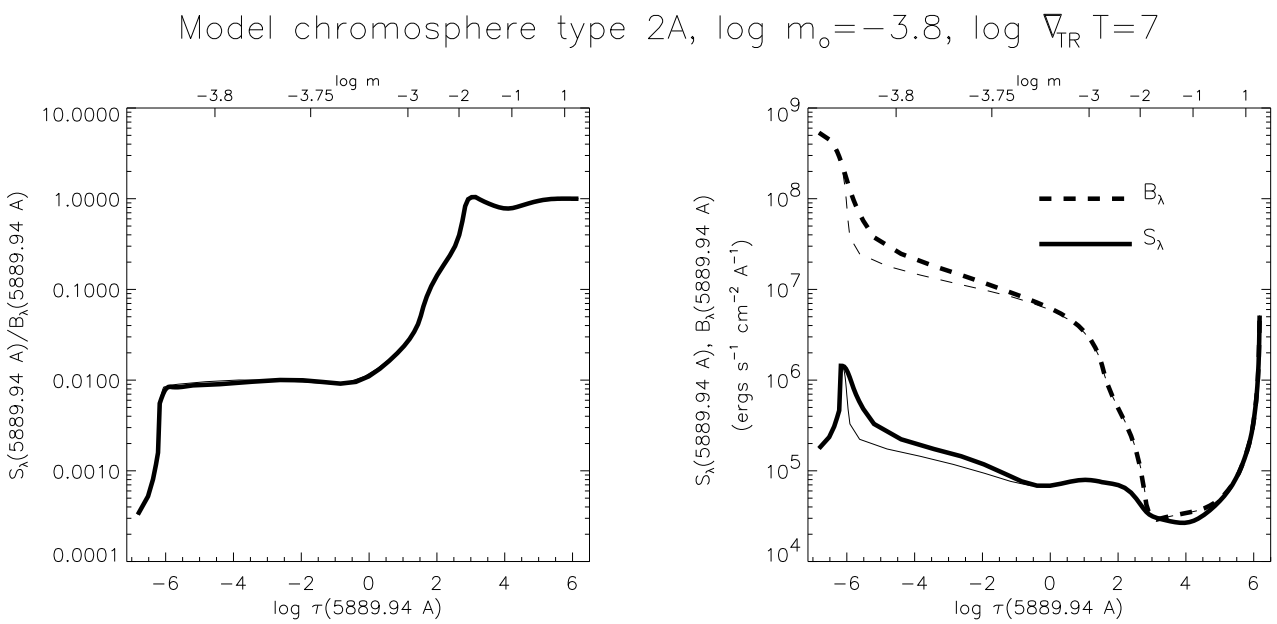

Fig. 11. Run of the source function and of the Planck function at the central wavelength of the D_2 component of the sodium doublet. The model chromosphere is the same as in Fig. 10. As in that figure, thinner lines represents quantities calculated accounting for the XUV coronal flux.

ering an XUV flux incident atop the model atmosphere. Significant changes occur in the core of the D lines in the presence of a strong XUV flux illuminating the chromosphere.

A closer inspection of specific models can give further insights on the physical process behind the emerging profiles. The alterations in the Na ionic equilibrium, shown in Fig. 10, are of particular interest. Clearly, over-ionisation of Na^+ will propagate through the recombination chain to Na^0. Fig. 10 also shows how the changes in the sodium ionisation equilibrium can reach the formation region of the D_2 core, if marginally.

As for the effect on the emerging profile of the D doublet, it is not easy to produce a simple quantitative model. Even limiting ourselves to the most active models, where the coupling of the line source function with the local Planck function is strongest, one should be aware that some of the relevant quantities vary considerably over the large region of line formation. However, in qualitative terms only, it is still possible to identify two possible effects.

The first possibility concerns the dependence on density of the emission cores we have noticed in Sect. 3.1.1 and Sect. 3.1.2. This density dependence is mainly due to the collisional coupling parameter ε of Eq. 1. Even if ε is in itself not constant throughout the line-forming region, the ratio between the source function and the Planck function is mainly determined by some "mean" value of ε (Athay 1972, p. 48). Notably, the surface value of the source function (closely related to the line-center emerging intensity) will be proportional to $<\varepsilon>^{1/2}$. The Na^+ ionisation front induced by coronal radiation will push down the upper boundary of the region where Na I chromospheric emission is produced, towards lower temperatures and electron densities. Consequently, $<\varepsilon>$ will decrease, causing a lower intensity in the line core.

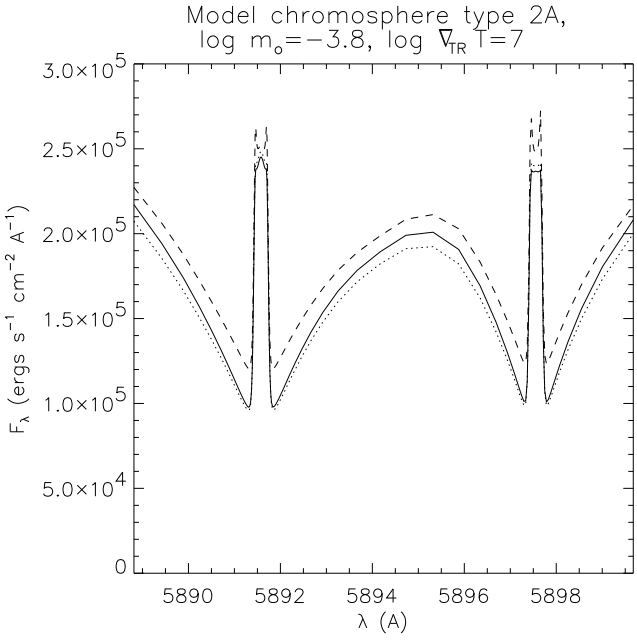

Fig. 12. Effect of collisions with hydrogen on the D profiles obtained with model chromosphere type 2A, $\log m_\circ = -3.8$ and $\log \nabla_{TR}\, T = 7$. The solid line is the "standard" calculations, i.e. Na-H collisions computed with Kaulakys cross-sections. The dotted line is the profile obtained neglecting collisions with hydrogen. The dashed line refers to calculations performed using the Drawin formulae.

The other possibility stems from the dependence of the emission cores on the thickness of the chromosphere (Sect. 3.1.2). In this case, an overionisation of Na^0 would in effect result in a reduction of the thickness of the chromosphere as seen by the D lines. Physically, the coronal photoionisation flux depletes the

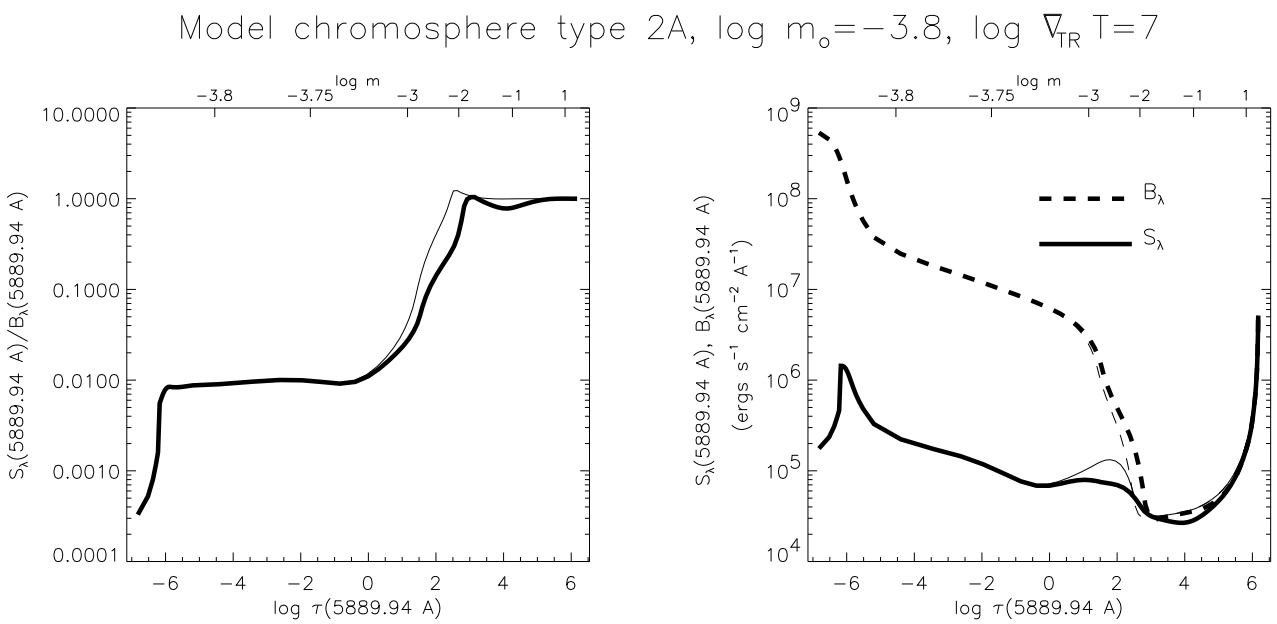

Fig. 13. Run of the source function and of the Planck function at the central wavelength of the D_2 component of the sodium doublet, as in Fig. 11. The thinner line refers to quantities obtained with Drawin cross-sections for H-Na collisions, the thicker lines refer to Kaulakys rates.

topmost layers of neutral sodium, thus exposing lower, cooler chromospheric layers. Again, the effect is a reduced core emission intensity.

To ascertain to what extent these two processes are effective, we examine in one particular model, as an example, the behaviour of the source function of the D_2 line (Fig. 11). An inspection of the left-hand panel of Fig. 11 reveals that in reality the ratio $S_\lambda/B_\lambda(T)$, as function of the optical depth, hardly changes in the presence of photoionising photons. The two curves in the left-hand panel of Fig. 11 are indeed practically indistinguishable. This rules out the first possible effect, the reduction of $<\varepsilon>$. In fact, since the region of formation of the line, i.e. the region where $<\varepsilon>$ is set, lies quite deep in the atmosphere, far more substantial XUV fluxes would be required to have an effect this way.

The dominant effect seems to be instead the lowering of the upper boundary of the "sodium chromosphere". This fact is clearly evident in the right hand panel of Fig. 11: at a given optical depth, the value of the Planck function in the chromosphere (and therefore of the source function) is lower in the presence of coronal illumination.

3.3. The effect of collisions with hydrogen

Another important issue is whether collisions with hydrogen can have a significant effect on the Na I D line profile. Fig. 12 addresses this problem, showing the inner profile of the doublet obtained in the usual "reference" active model we have considered in the previous sections. It is clear that the inclusion of the Kaulakys rates does not appreciably change the cores, and only has a limited influence on the upper photospheric profile. Note, in particular, the change in the region where the wings of the two components overlap.

On the other hand, the Drawin rates do produce more significant changes, even in the cores. But, considering that those rates are as much as two or three orders of magnitude larger, the changes are surprisingly small. As for the emission core, it forms in the chromosphere, where hydrogen starts to release more electrons. Therefore it is reasonable to expect that electron collisional rates are not easily overwhelmed in that region. The relatively small effect on the deeper parts of the line profile can instead be justified by considering that in those regions departures from LTE are not very strong. Thus, since adding any further thermalisation process brings the source function closer to LTE, the changes are relatively modest.

Fig. 13, the analogue of Fig. 11, quite clearly illustrates this point. In fact the thermalisation depth (the depth where the source function approaches LTE) changes when using Drawin instead of Kaulakys rates. But over much of the chromosphere there is little or virtually no change. Nevertheless, the particular choice of the collisional rates does have consequences on the source function in the temperature minimum region and lower chromosphere.

3.4. Dependence on background opacity

Finally, it is interesting to examine the effect of the choice of background opacities on the calculated line profiles. Fig. 14 shows the effect of neglecting plasma background line opacities on the visible and infrared chromospheric diagnostics considered in this work.

It should once more be stressed that the low wavelength resolution (2 Å) of the original opacity table adopted here is not suitable for comparisons with high resolution data. However, the chromospheric cores of the strong lines we have considered are affected relatively little by these computational details. A

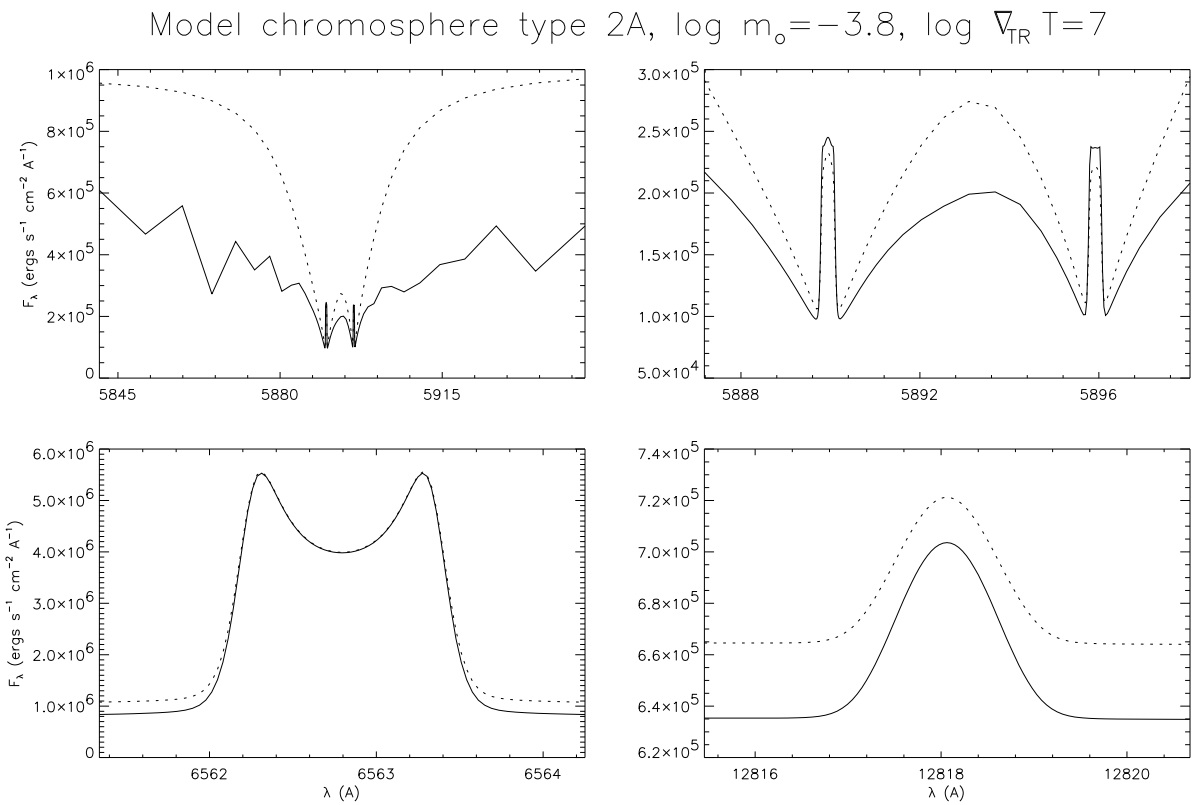

Fig. 14. The D doublet (upper panels), Hα (lower-left panel) and Paβ (lower-right panel) computed taking into account background line opacities (solid lines) or continuum opacities only (dotted line). All the calculations were made for model chromosphere type 2A, $\log m_\circ = -3.8$ and $\log \nabla_{\rm TR}\, T = 7$.

major effect is instead seen in the wings of the D lines: it is clear that any comparison with observations of cool stars cannot exclude a realistic treatment of the background opacity. This is especially important if the sensitivity of the D lines to the lower chromosphere, demonstrated in Sect. 3.1, is to be exploited.

Similar considerations on the importance of a proper treatment of background opacities in theoretical modelling, can be extended to other chromospheric diagnostics as well. In general, the theoretical "continuum" fluxes computed neglecting atomic and molecular line absorption in the photosphere of cool stars are overestimates. This fact may impair the correct evaluation of the source function of the chromospheric diagnostics. But even for a collisionally dominated line, such as Hα in the most active models, the level of the continuum is important for comparing synthetic spectra with observed profiles. Unless the line is optically thin, its chromospheric emission is not just superimposed on the photospheric background: the computed *relative* profile will then depend on the accuracy of the computed photospheric flux. A comparison between Hα and Paβ in Fig. 14 is sufficient to illustrate this point.

4. Conclusions

We have investigated the potential of the Na I D doublet as chromospheric diagnostics in a cool dwarf of $T_{\rm eff}$ = 3700 K, $\log g$ = 4.7 and solar metallicity. Using an extended grid of model chromospheres, we have computed both H I and Na I non-LTE spectra in a variety of situations corresponding to a broad span of chromospheric activity.

From a comparison of the spectra of the two elements, we have shown that the information to be gathered from the D lines can effectively complement that obtained with other diagnostics, such as Hα or Paβ. In particular, confirming previous investigations, we find that H I lines are chiefly sensitive to the structure of the upper chromosphere–lower transition region. In contrast, our calculations indicate that the cores of the D lines are nearly insensitive to the structure of the lower transition region, while being a good probe of the conditions in the middle-to-lower chromosphere.

Moreover, while the H I lines, when in emission, seem to depend mainly on the the *density* of the upper chromosphere and/or lower transition region, the emission cores of the D lines appear to depend *both on the density and on the thickness* of the chromosphere. For example, at a given chromospheric density, the extension of the chromosphere can have a large effect on the amount of inner-core self-absorption.

We have also pointed out how the Na ionisation equilibrium and, consequently, the emerging D-line profile can be affected by the presence of an active corona. The coronal radiation acts on the Na I lines mainly via the dependence of the emission core

on the optical thickness of the chromosphere in the D doublet. This effect is normally not important, but may be significant for very active stars.

Another effect that should be accounted for in cool atmospheres, is the additional thermalisation due to inelastic collisions with hydrogen. We have included this effect in all our calculations, using a formula appropriate for Rydberg atoms. We have showed that the inclusion of such collision rates can only marginally alter the Na I D line profiles in the models we have considered. To some extent, this remains true even if the alternative, probably overestimated Drawin cross-sections are adopted. This is because much of the line profile is formed in regions where departures from LTE are not dramatic, while the inner cores form in regions where the electron density is high enough to reduce the importance of collisions with hydrogen.

Finally, we have included the effect of the severe atomic and molecular line haze in so cool an atmosphere by suitably adapting to our grid of chromospheres a model-specific opacity table. This has enabled us to estimate the importance of a realistic treatment of photospheric background opacities. The effect is especially important in the broad damping wings of the D doublet, but it is not negligible even in the emission cores produced by the most active models.

Acknowledgements. The main body of this work has been carried out at Armagh Observatory, supported by PPARC grant GR/K04613. We acknowledge support at Armagh in terms of both software and hardware by the STARLINK Project, funded by the UK PPARC. The work was completed while one of the authors (V. A.) held a National Research Council-NASA/GSFC Research Associateship at Goddard Space Flight Center.

We are indebted with P. Hauschildt and F. Allard for computing the model photosphere and the opacity table used as a base for our calculations. We are also grateful to G. Severino for providing the Na-H collisional rates, as well for a number of valuable and stimulating discussions.

We wish to thank S. D. Jordan for his useful comments on the manuscript.

References

Allard, F., Hauschildt, P. H., 1995a, ApJ, 445, 433
Allard, F., Hauschildt, P. H., 1995b, private communication
Andretta, V., Giampapa, M. S., 1995, ApJ, 439, 405
Athay, R. G., 1972, Radiation Transport in Spectral Lines (Dordrecht: Reidel)
Avrett, E. H., Loeser, R., 1988, ApJ, 331, 211
Bruls, J. H. M. J., Rutten, R. J., Shchukina, N. G., 1992, A&A, 265, 237
Caccin, B., Gomez, M. T., Severino, G., 1993, A&A, 276, 219
Carlsson, M., 1986, Uppsala Observatory Internal Report no. 33
Cram, L. E., 1982, ApJ, 253, 768
Cram, L. E., Mullan, D. J., 1979, ApJ, 234, 579
Cram, L. E., Mullan, D. J., 1985, ApJ, 294, 626
Doyle, J. G.., Butler, C. J., 1985, Nat, 313, 378
Drawin, H. W.., 1968, Z. Physik, 211, 404
Drawin, H. W.., 1969, Z. Physik, 225, 470
Houdebine, E. R., Doyle, J. G., 1994, A&A, 289, 169
Johnson, L. C., 1972, ApJ, 174, 227
Kaulakys, B., 1985, J. Phys. B, 18, L167
Kaulakys, B., 1986, Sov. Phys. JEPT, 64, 229
Kelch, W. L., Milkey, R. W., 1976, ApJ, 208, 428
Landini, M., Monsignori Fossi, B. C., 1990, A&AS, 82, 229
Magain, P., 1986, A&A, 163, 135
Panagi, P. M., Byrne, P. B., Houdebine, E. R., 1991, A&AS, 90, 437
Pavlenko, Y. V., Magazzù, A., 1996, A&A, 311, 961
Pettersen, B. R., 1989, A&A, 209, 279
Pettersen, B. R., Hawley, S. L., 1989, A&A, 217, 187
Sakhibullin, N. A., 1987, SvA, 31, 666
Seaton, M. J., 1987, J. Phys. B, 20, 6363
Scott, M. P., 1996, to be published
Steenbock, W., Holweger, H., 1984, A&A, 130, 319
Thatcher, J. D., 1994, Ph. D. Thesis, Univ. of Sydney
Thomas, R. N., 1957, ApJ, 125, 260
Thomas, R. N., 1965, Some Aspects of Non-Equilibrium Thermodynamics in the Presence of a Radiation Field, Univ. of Colorado Press, Boulder, p. 174
Tobiska, W. K., 1991, J. Atmos. Terr. Phys., 53, 1005
Vernazza, J. E., Avrett, E. H., Loeser, R., 1981, ApJS, 45, 635

This article was processed by the author using Springer-Verlag LaTeX A&A style file *L-AA* version 3.